JACS
JOURNAL OF THE AMERICAN CHEMICAL SOCIETY

Communication

Direct In Situ Raman Spectroscopic Evidence of Oxygen Reduction Reaction Intermediates at High-Index Pt(hkl) Surfaces

Jin-Chao Dong, Min Su, Valentin Briega-Martos, Lang Li, Jia-Bo Le, Petar Radjenovic, Xiao-Shun Zhou, Juan Miguel Feliu, Zhong-Qun Tian, and Jian-Feng Li

J. Am. Chem. Soc., **Just Accepted Manuscript** • DOI: 10.1021/jacs.9b12803 • Publication Date (Web): 30 Dec 2019

Just Accepted

is published by the American Chemical Society. 1155 Sixteenth Street N.W., Washington, DC 20036

Direct *In Situ* Raman Spectroscopic Evidence of Oxygen Reduction Reaction Intermediates at High-Index Pt(*hkl*) Surfaces

Jin-Chao Dong[†#], Min Su[†#], Valentín Briega-Martos[‡], Lang Li[†], Jia-Bo Le[†], Petar Radjenovic[†], Xiao-Shun Zhou[§], Juan Miguel Feliu[‡,*], Zhong-Qun Tian[†], Jian-Feng Li[†,*]

[†] State Key Laboratory of Physical Chemistry of Solid Surfaces, iChEM, College of Chemistry and Chemical Engineering, College of Energy, Xiamen University, Xiamen 361005, China.

[‡] Instituto de Electroquímica, Universidad de Alicante, Alicante E-03080, Spain.

[§] Key Laboratory of the Ministry of Education for Advanced Catalysis Materials, College of Chemistry and Life Sciences, Zhejiang Normal University, Jinhua 321004, China

Supporting Information Placeholder

ABSTRACT: The study of the oxygen reduction reaction (ORR) at high-index Pt(*hkl*) single crystal surfaces has received considerable interest due to their well-ordered, typical atomic structures and superior catalytic activities. However, it is difficult to obtain direct spectral evidence of ORR intermediates during reaction processes, especially at high-index Pt(*hkl*) surfaces. Herein, *in situ* Raman spectroscopy has been employed to investigate ORR processes at high-index Pt(*hkl*) surfaces containing the $[01\bar{1}]$ crystal zone – i.e. Pt(211) and Pt(311). Through control and isotope substitution experiments, *in situ* spectroscopic evidence of OH and OOH intermediates at Pt(211) and Pt(311) surfaces was successfully obtained. After detailed analysis based on the Raman spectra and theoretical simulation, it was deduced that the difference in adsorption of OOH at high-index surfaces has a significant effect on the ORR activity. This research illuminates and deepens the understanding of the ORR mechanism on high-index Pt(*hkl*) surfaces and provides theoretical guidance for the rational design of high activity ORR catalysts.

In fundamental research, the surface structure of the catalysts is known to have a crucial effect on the reaction processes and the adsorption of intermediate species. Research on reaction processes at atomically flat and well-defined single crystal surfaces acts as a bridge between experimental observations and theoretical simulations and provides unparalleled insights.[1-4] Compared with low-index single crystal surfaces, high-index single crystal surfaces generally have better catalytic activities, with more accessible surface structures and lower atomic coordination numbers, facilitating better interactions with interfacial reactants or reaction intermediates.[5-9] Therefore, studying the facet effects of different high-index surface structures has important practical significance for understanding interfacial catalytic mechanisms and guiding the rational design of catalysts.

As the most important cathode reaction in fuel cells, research on the oxygen reduction reaction (ORR) mechanism at Pt(*hkl*) surfaces has long been of interest to the scientific and catalysis communities,[10-13] with traditional electrochemical methods being commonly used to study ORR processes on different Pt(*hkl*) surfaces.[14-17] Compared with the Pt(111) and Pt(100) surfaces which are the flattest low-index crystal surfaces, high-index Pt(*hkl*) surfaces have different degrees of terraces and step densities with Pt(211) having the best ORR activity. Interestingly, ORR activity usually increases with an increase in step density in the $[01\bar{1}]$ stepped crystal zone. However, though the step density of Pt(311) is higher than Pt(211), its activity is slightly lower than Pt(211).[18] This trend may be due to the different adsorption free energies of ORR intermediates at Pt(211) and Pt(311) surface, but the exact reasons are still uncertain.

Since knowledge of the exact reaction mechanisms, intermediates and their adsorption configurations generated at different surfaces is difficult to precisely attain using conventional electrochemical techniques, spectroscopic methods have been used to qualitatively observe interfacial processes. For example, infrared (IR) and surface-enhanced Raman spectroscopy (SERS) have been used to study ORR processes at different polycrystalline electrode surfaces, providing *in situ* spectral evidence of different ORR intermediate species.[19-23] However, most previous spectroscopic studies have been unsuitable for directly studying the ORR on single crystal surfaces at the atomic level in aqueous systems. The invention of shell-isolated nanoparticle-enhanced Raman spectroscopy (SHINERS) by our group has allowed enhanced Raman signals from different surfaces, especially single crystal surfaces to be collected effectively.[24] Additionally, SHINERS has been successfully

applied to study various molecular adsorption and electrode catalytic processes on different low-index single crystal surfaces.[25-28] Herein, considering their unique crystal structures and higher ORR activities, *in situ* SHINERS was employed to study ORR processes (Figure 1 and Figure S1) at Pt(311) and Pt(211) surfaces, to observe and understand the ORR mechanism on high-index Pt(*hkl*) surfaces.

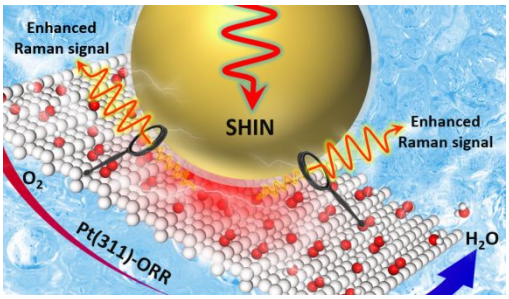

Figure 1. Schematic of SHINERS study of the ORR at Pt(311) surface. The golden sphere with a transparent silica shell represents the SHIN (Au@SiO2), the enhancement hot spot is highlighted in red, the red-yellow arrows depict the laser signal. The big white, small white and red spheres represent Pt, H and O atoms, respectively.

For the cyclic voltammogram (CV) of Pt(111) in 0.1 M $HClO_4$ solution saturated with Ar (Figure 2a - black curve), the low potential region between 0.05 - 0.25 V corresponds to absorption and desorption of "H_{ad}", and the complex CV signal between 0.6 - 0.85 V is attributed to the reversible formation of "OH_{ad}".[29-30] For Pt(211) and Pt(311) surfaces (Figure 2a - red and blue curves, respectively), the peaks between 0.05 - 0.2 V are the absorption/desorption of "H" at terrace sites, and the peaks between 0.2 -0.4 V represent the anion and/or "H" absorption/desorption features on (111) - (100) step-terrace sites.[31] At potentials below 0.9 V (Figure S2) the surface order is well maintained for both Pt(211) and Pt(311), however higher potential limits result in changes in the H_{upd} region, implying some disordering due to oxidation. The ORR activity of these three facets was then investigated. In Figure 2b, the ORR onset potentials on the three surfaces start at ~ 1.0 V (Figure S3 and Figure S4). From the half-slope potential point in Figure 2b, the ORR activities on the three electrodes follow the order: Pt(111) ≈ Pt(211) > Pt(311), in 0.1 M $HClO_4$. Also, if the initial potential of ORR on three surfaces is ≤ 0.9 V (Figure S5 and Figure S6), the ORR activities follow the order: Pt(211) > Pt(111) > Pt(311), which matches previous work.[18] However, in this system, Pt(211) and Pt(311) have a certain degree of oxidation at the initial ORR potential (~ 1.0 V), leading to a partial disordering in the crystal surfaces and resulting in slightly different ORR activities.

In situ electrochemical SHINERS was then used to investigate the ORR at the Pt(311) surface, and the SHINs only has a negligible effect on the electrochemistry and ORR activity of Pt(*hkl*) surfaces (Figure S7). As shown in Figure 2c, at initial potentials no significant Raman peaks are visible other than a peak at 933 cm^{-1} belonging to bulk $HClO_4$ in solution. As the potential decreases, a pair of Raman peaks, around 1040 cm^{-1} and 765 cm^{-1}, appear at 0.9 V. Further decreasing the potential causes the Raman peak around 1040 cm^{-1} to become slightly stronger, while the Raman peak of 765 cm^{-1} remains stable regardless the potential. Generally, the OH species adsorbed or desorbed on Pt(*hkl*) surfaces in Ar saturated solution, which originates from breakage of water molecules on Pt(*hkl*) surface. However, in the control experiment saturated with Ar (Figure 2d), the peaks at 1040 cm^{-1} and 765cm^{-1} are not observed, indicating that they are related to ORR processes. Based on previous research on low-index Pt(*hkl*) surfaces,[28] the Raman peak around 1040 cm^{-1} is possibly associated with either OH or superoxide species, while the peak at 765 cm^{-1} is likely associated with a peroxide species. We then carried out some isotopic experiments to qualify these spectral bands.

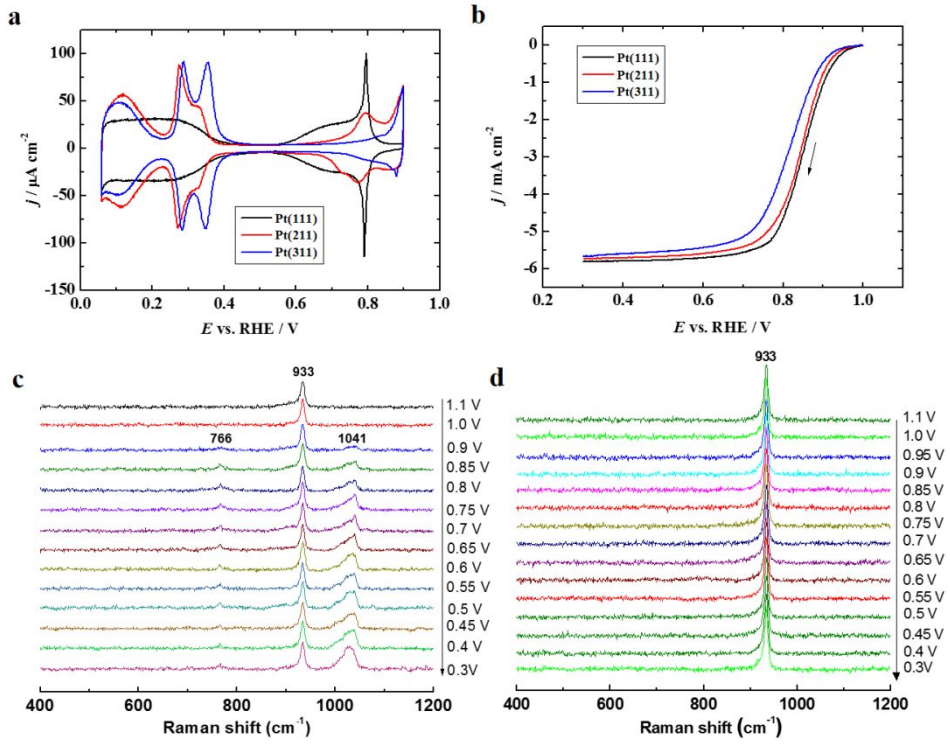

Figure 2. a) Electrochemical results of Pt(*hkl*) surfaces in 0.1 M $HClO_4$ solution saturated with Ar and **b)** saturated with O_2, respectively, with 1600 rpm. rotation rate, scan rate = 50 mV/s; **c)** SHINERS spectra of Pt(311) surface in 0.1 M $HClO_4$ solution saturated with O_2 and **d)** with Ar), respectively.

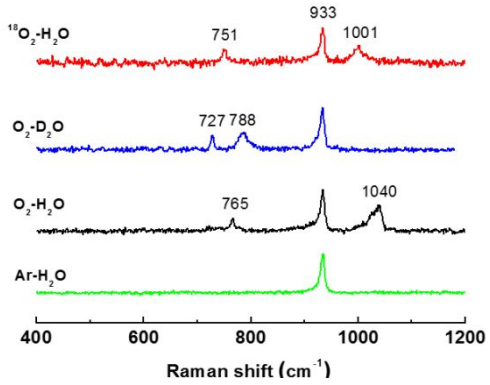

Figure 3. Isotopic control spectra for ORR processes on the Pt(311) surface under different conditions in aqueous and deuterated 0.1 M $HClO_4$ solutions under 0.7 V.

In deuterated experiments, it was found that the Raman peaks around 1040 cm^{-1} and 765 cm^{-1} were significantly shifted to lower wavenumbers, with the peak at 1040 cm^{-1} shifting to around 788 cm^{-1} and the peak at 765 cm^{-1} shifting to 727 cm^{-1} (Figure 3 - blue curve). Indicating that both of these peaks are associated with the "H" atom. The Raman frequency ratio in isotopic experiment to that in normal experiment can be approximately analyzed by the mass formulas (Formula S1-S4). Regarding the species with the peak at 1040 cm^{-1}, such a large shift in the D2O experiments indicates "OH" species. Previous research has shown that the peroxide species should appear in the range between 700-900 cm^{-1}.[20,22,32,33] As the peak around 765 cm^{-1} shifted to a lower wavenumber in D2O experiments, this indicates proton interactions and thus corresponds to "OOH" species. For further verification, $^{18}O_2$ isotope experiments were also performed and found that the peak at 1040 cm^{-1} shifted to around 1001 cm^{-1}, while the peak of 765 cm^{-1} slightly shifted to 751 cm^{-1} (Figure 3 - red curve). Suggesting both of these peaks are related to the "O" atom.

In previous study, the OOH species appeared around 735 cm^{-1} at the Pt(111) surface and the OH species appeared around 1080 cm^{-1} at the Pt(100) surface.[28] Comparing these peaks on low-index surfaces with those observed herein on Pt(311), there are obvious shifts in the Raman frequencies between surfaces. This can be accounted for by the difference in the surface structure of Pt(311) compared with low-index Pt(*hkl*) surfaces which will affect the adsorption configuration or adsorption energy of surface species. Therefore, for the Pt(311) surface the 1040 cm^{-1} peak can be ascribed to an adsorbed OH species, while the peak of 765 cm^{-1} corresponds to OOH species. Similar to the Pt(311) surface, a pair of Raman peaks at 1040 cm^{-1} and 765 cm^{-1} appear at ORR potentials at the Pt(211) surface (Figure 4a) and are assigned to OH and OOH surface species, respectively (Figure S8). However, there is a slight difference in the ORR profiles between Pt(211) and Pt(311). For the Pt(211) surface, both Raman peaks around 1040 cm^{-1} and 765 cm^{-1} only appear at potentials below 0.9 V and first increase with decreasing potential, then weaken after reaching a maximum at about 0.7 V. This indicates that the surface concentration of OOH and OH species changed significantly during the ORR process at the Pt(211) surface. Compared to the low-index Pt(*hkl*) surfaces, the presence of both the OOH and OH species simultaneously in the Raman spectra of the high-index crystal surfaces (Figure 4b), further demonstrating the surface sensitivity of ORR intermediate species to the single crystal surface structure.

Based on the SHINERS and electrochemical results, a higher adsorption energy for the OOH intermediate at the Pt(311) surface is likely the main reason for its lower reactivity than the Pt(211) surface.[15,18,34] Considering the SHINERS results, the Raman band around 765 cm^{-1} at the Pt(311) surface for the adsorbed OOH is considerably more intense than for Pt(211) (Figure 2c and 4), despite the latter surface having longer terraces. The lower intensity of the OOH peak at the Pt(211) surface could be due to OOH not being bonded to the surface as strongly as at Pt(311) surface, and therefore it could more readily desorb and diffuse along the surface to react at other (111) or (100) sites. The stronger adsorption energy in the case of Pt(311) would account for the higher intensity of the Raman band, and also for its lower activity, since the strongly adsorbed OOH intermediate would be more stable than in the case of longer terraces, and equilibrium with the species in solution is more favored.[16] Meanwhile, the OOH peak around 735 cm^{-1} for Pt(111) is much more intense than for the Pt(211) and Pt(311) surfaces (Figure 4b) because in this case the terraces are very long, so the amount of adsorbed OOH species

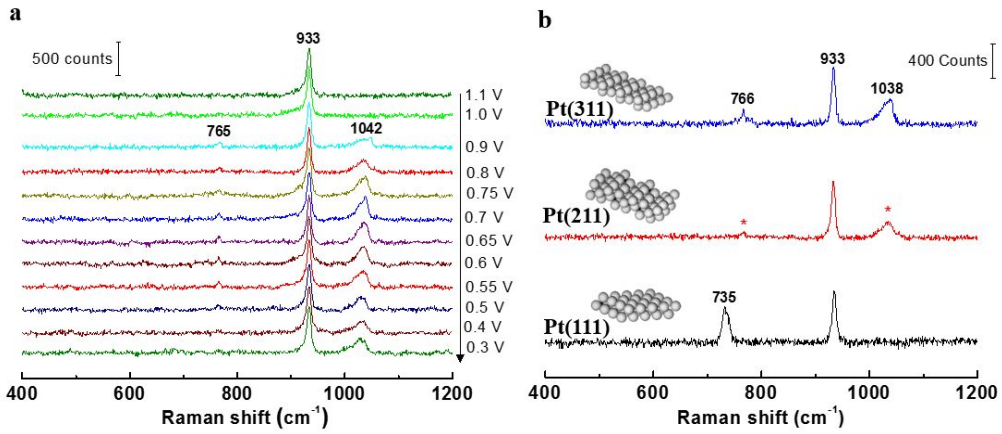

Figure 4. a) SHINERS of ORR at Pt(211) in 0.1 M $HClO_4$ solution; **b)** SHINERS of different Pt(*hkl*) surfaces in 0.1 M $HClO_4$ solution (saturated with O_2) at 0.8 V held potential (normalized with the solution peak of 933 cm^{-1}).

would be very high. The higher adsorption energy of the adsorbed OOH intermediate at the Pt(311) surface can be further justified by considering the electrochemical behaviour (Figure 2 a-b). Currents at the lowest potentials correspond to the H adsorption/desorption region at the (111) terraces and also to hydrogen and OH adsorption/desorption at steps. The voltammetric profile in this potential region is considerably modified when comparing Pt(211) and Pt(311) (see Figure 2a between 0.06 and 0.4 V). This indicates changes in the adsorption energies of H and OH species, and one could expect also changes in the adsorption energies of OOH intermediate since the chemical nature is very similar. To further confirm these conclusions, density functional theory (DFT) was employed to investigate the adsorption state of OOH on Pt(311) and Pt(211) surfaces. It was found that the adsorption energy of OOH on Pt(311) surface is indeed higher than Pt(211) surface(Figure S9 - 10, Table S1), which correlates well with our conclusions.

In summary, *in situ* Raman spectroscopic evidence of the key ORR intermediates, OH and OOH, was obtained for the first time at high-index Pt(*hkl*) surfaces. A series of control and isotope substitution experiments were performed to confirm the characterization of these spectral peaks. It was shown that the high ORR activity of high-index Pt(*hkl*) surfaces are due to the interfacial reaction characteristics of various surface structures and also the different adsorption energy of intermediates on different surfaces related to synergistic facet effect of specific surface structures likely also plays an important part. Also, the specific adsorption of different intermediates on different surfaces is the cause of the higher ORR activity of Pt(211) than Pt(311). Therefore, it is possible to design new catalysts with different crystal surface structures to achieve higher ORR catalytic activity with compound characteristics of different single crystal facets. This also provides theoretical guidance for the preparation of high-efficiency ORR catalysts.

ASSOCIATED CONTENT

Supporting Information

Experimental section, supporting results, electrochemical, *in situ* SHINERS experiments and DFT calculations for Figure S1-S10, Formula S1-S4 and Table S1. The Supporting Information is available free of charge on the ACS Publications website.

AUTHOR INFORMATION

Corresponding Author

Li@xmu.edu.cn, juan.feliu@ua.es

Author Contributions

[#]J. C. D. and M. S. contributed equally.

Notes

The authors declare no competing financial interests.

ACKNOWLEDGMENT

This work was financially supported by the National Natural Science Foundation of China (21902137, 21925404, 21775127, and 21427813), the Fundamental Research Funds for the Central Universities (20720190044), the China Postdoctoral Science Foundation (2019M652250), China Postdoctoral Innovation Talent Support Program (BX20190184). Support from MINECO through project CTQ2016-76221-P (AEI/FEDER, UE) is greatly acknowledged.

REFERENCES

(1) Huang, L.; Zhang, X.; Wang, Q.; Han, Y.; Fang, Y.; Dong, S. Shape-control of Pt–Ru nanocrystals: tuning surface structure for enhanced electrocatalytic methanol oxidation. *J. Am. Chem. Soc.* **2018**, *140(3)*, 1142-1147.

(2) Nunez, M.; Lansford, J. L.; Vlachos, D. G. Optimization of the facet structure of transition-metal catalysts applied to the oxygen reduction reaction. *Nat. Chem.* **2019**, *11*, 449-456.

(3) Seh, Z. W.; Kibsgaard, J.; Dickens, C. F.; Chorkendorff, I.; Nørskov, J. K.; Jaramillo, T. F. Combining theory and experiment in electrocatalysis: Insights into materials design. *Science* **2017**, *355*, eaad4998.

(4) Wang, C.; Chen, X.; Chen, T. M.; Wei, J.; Qin, S. N.; Zheng, J. F.; Zhang, H.; Tian, Z. Q.; Li, J. F. In-situ SHINERS study of the size and composition effect of Pt-based nanocatalysts in catalytic hydrogenation. *ChemCatChem* **2019**, doi: 10.1002/cctc.201901747.

(5) García, G.; Stoffelsma, C.; Rodriguez, P.; Koper, M. T. Influence of beryllium cations on the electrochemical oxidation of methanol on stepped platinum surfaces in alkaline solution. *Surf. Sci.* **2015**, *631*, 267-271.
(6) McCrum, I. T.; Chen, X.; Schwarz, K. A.; Janik, M. J.; Koper, M. T. Effect of step density and orientation on the apparent pH dependence of hydrogen and hydroxide adsorption on stepped platinum surfaces. *J. Phys. Chem. C* **2018**, *122*, 16756-16764.
(7) Chen, X.; McCrum, I. T.; Schwarz, K. A.; Janik, M. J.; Koper, M. T. M. Co-adsorption of cations as the cause of the apparent pH dependence of hydrogen adsorption on a stepped platinum single-crystal electrode. *Angew. Chem. Int. Ed.* **2017**, *56*, 15025-15029.
(8) Luo, M.; Sun, Y.; Zhang, X.; Qin, Y.; Li, M.; Li, Y.; Li, C.; Yang, Y.; Wang, L.; Gao, P.; Lu, G.; Guo, S. Stable high-index faceted Pt skin on zigzag-like PtFe nanowires enhances oxygen reduction catalysis. *Adv. Mater.* **2018**, *30*, 1705515.
(9) Tian, N.; Zhou, Z. Y.; Sun, S. G.; Ding, Y.; Wang, Z. L. Synthesis of tetrahexahedral platinum nanocrystals with high-index facets and high electro-oxidation activity. *Science* **2007**, *316*, 732-735.
(10) Kulkarni, A.; Siahrostami, S.; Patel, A.; Norskov, J. K. Understanding catalytic activity trends in the oxygen reduction reaction. *Chem. Rev.* **2018**, *118*, 2302-2312.
(11) Kumeda, T.; Tajiri, H.; Sakata, O.; Hoshi, N.; Nakamura, M. Effect of hydrophobic cations on the oxygen reduction reaction on single-crystal platinum electrodes. *Nat. Commun.* **2018**, *9*, 4378.
(12) Damjanovic, A.; Brusic, V. Electrode kinetics of oxygen reduction on oxide-free platinum electrodes. *Electrochim. Acta* **1967**, *12*, 615-628.
(13) Nørskov, J. K.; Rossmeisl, J.; Logadottir, A.; Lindqvist, L.; Kitchin, J. R.; Bligaard, T.; Jonsson, H. Origin of the overpotential for oxygen reduction at a fuel-cell cathode. *J. Phys. Chem. B* **2004**, *108*, 17886-17892.
(14) Markovic, N. M.; Gasteiger, H. A.; Ross, Jr., P. N. Oxygen reduction on platinum low-index single-crystal surfaces in sulfuric acid solution: rotating ring-Pt (hkl) disk studies. *J. Phys. Chem.* **1995**, *99*, 3411-3415.
(15) Gómez-Marín, A. M.; Rizo, R.; Feliu, J. M. Oxygen reduction reaction at Pt single crystals: a critical overview. *Catal. Sci. Technol.* **2014**, *4*, 1685-1698.
(16) Briega-Martos, V.; Herrero, E.; Feliu, J. M. Effect of pH and water structure on the oxygen reduction reaction on platinum electrodes. *Electrochim. Acta* **2017**, *241*, 497-509.
(17) Ruge, M.; Drnec, J.; Rahn, B.; Reikowski, F.; Harrington, D. A.; Carla, F.; Felici, R.; Stettner, J.; Magnussen, O. M. Structural reorganization of Pt (111) electrodes by electrochemical oxidation and reduction. *J. Am. Chem. Soc.* **2017**, *139*, 4532-4539.
(18) Maciá, M. D.; Campiña, J. M.; Herrero, E.; Feliu, J. M. On the kinetics of oxygen reduction on platinum stepped surfaces in acidic media. *J. Electroanal. Chem.* **2004**, *564*, 141-150.
(19) Nayak, S.; McPherson, I. J.; Vincent, K. A. Adsorbed intermediates in oxygen reduction on platinum nanoparticles observed by in situ IR spectroscopy. *Angew. Chem. Int. Ed.* **2018**, *57*, 12855-12858.
(20) Wang, Y. H.; Le, J. B.; Li, W. Q.; Wei, J.; Radjenovic, P.; Zhang, H.; Zhou, X. S.; Cheng, J.; Tian, Z. Q.; Li, J. F. *In situ* spectroscopic insight into the origin of the enhanced performance of bimetallic nanocatalysts towards ORR. *Angew. Chem. Int. Ed.* **2019**, *58*, 16062-16066.
(21) Johnson, L.; Li, C.; Liu, Z.; Chen, Y.; Freunberger, S. A.; Ashok, P. C.; Praveen, B. B.; Dholakia, K.; Tarascon, J. M.; Bruce, P. G. The role of LiO_2 solubility in O_2 reduction in aprotic solvents and its consequences for Li-O_2 batteries. *Nat. Chem.* **2014**, *6*, 1091-1099.
(22) Shao, M. H.; Liu, P.; Adzic, R. R. Superoxide anion is the intermediate in the oxygen reduction reaction on platinum electrodes. *J. Am. Chem. Soc.* **2006**, *128*, 7408-7409.
(23) Li, X.; Gewirth, A. A. Oxygen electroreduction through a superoxide intermediate on Bi-modified Au surfaces. *J. Am. Chem. Soc.* **2005**, *127*, 5252-5260.
(24) Li, J. F.; Huang, Y. F.; Ding, Y.; Yang, Z. L.; Li, S. B.; Zhou, X. S.; Fan, F. R.; Zhang, W.; Zhou, Z. Y.; Wu D. Y.; Ren, B.; Wang, Z. L.; Tian, Z. Q. Shell-isolated nanoparticle-enhanced Raman spectroscopy. *Nature* **2010**, *464*, 392-395.
(25) Li, C. Y.; Le, J. B.; Wang, Y. H.; Chen, S.; Yang, Z. L.; Li, J. F.; Cheng, J.; Tian, Z. Q. In situ probing electrified interfacial water structures at atomically flat surfaces. *Nat. Mater.* **2019**, *18*, 697-701.
(26) Wang, Y. H.; Wei, J.; Radjenovic,P.; Tian, Z. Q.; Li, J. F. In situ analysis of surface catalytic reactions using SHINERS. *Anal. Chem.* **2019**, *91*, 1675-1685
(27) Li, C. Y.; Dong, J. C.; Jin, X.; Chen, S.; Panneerselvam, R.; Rudnev, A. V.; Yang, Z. L.; Li, J. F.; Wandlowski, T.; Tian, Z. Q. In situ monitoring of electrooxidation processes at gold single crystal surfaces using shell-isolated nanoparticle-enhanced Raman spectroscopy. *J. Am. Chem. Soc.* **2015**, *137*, 7648-7651.
(28) Dong, J. C.; Zhang, X. G.; Briega-Martos, V.; Jin, X.; Yang, J.; Chen, S.; Yang, Z. L.; Wu, D. Y.; Feliu, J. M.; Williams, C. T.; Tian, Z. Q.; Li, J. F. In situ Raman spectroscopic evidence for oxygen reduction reaction intermediates at platinum single-crystal surfaces. *Nat. Energy* **2019**, *4*, 60-67.
(29) Koper, M. T. M.; Lukkien, J. J. Modeling the butterfly: the voltammetry of ($\sqrt{3}\times\sqrt{3}$) R30 and p(2×2) overlayers on (111) electrodes. *J. Electroanal. Chem.* **2000**, *485*, 161-165.
(30) Berná, A.; Climent, V.; Feliu, J. M. New understanding of the nature of OH adsorption on Pt (111) electrodes. *Electrochem. Commun.* **2007**, *9*, 2789-2794.
(31) Marinković, N.M.; Adžić, R. Electrosorption of hydrogen and sulphuric acid anions on single-crystal platinum stepped surfaces: Part I. The [110] zone. *J. Electroanal. Chem.* **1988**, *241*, 309-328.
(32) Radjenovic, P. M.; Hardwick, L. J. Evaluating chemical bonding in dioxides for the development of metal–oxygen batteries: vibrational spectroscopic trends of dioxygenyls, dioxygen, superoxides and peroxides. *Phys. Chem. Chem. Phys.* **2019**, *21*, 1552-1563.
(33) Itoh, T.; Maeda, T.; Kasuya, A. In situ surface-enhanced Raman scattering spectroelectrochemistry of oxygen species. *Faraday Discuss.* **2006**, *132*, 95-109.
(34) Greeley, J.; Rossmeisl, J.; Hellman, A.; Nørskov, J. K. Theoretical trends in particle size effects for the oxygen reduction reaction. *Z. Phys. Chem.* **2007,** *221*, 1209-1220.

.

TOC Graphic

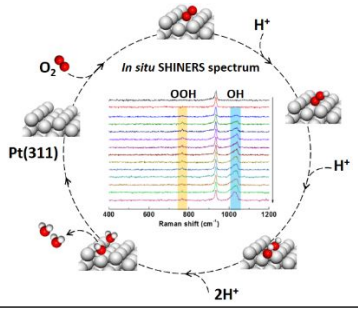
H+
O2
In situ SHINERS spectrum
OOH
OH
Pt(311)
H+
400
600
800
1000
1200
Raman shift (cm-1)
2H+